Microbial processes forming daily lamination in an aragonite travertine, Nagano-yu hot spring, Southwest Japan

Okumura, Tomoyo
Division of Evolution of Earth Environment, Graduate School of Social and Cultural Studies, Kyushu University

Takashima, Chizuru
Faculty of Culture and Education, Saga University

Shiraishi, Fumito
Division of Evolution of Earth Environment, Graduate School of Social and Cultural Studies, Kyushu University

Nishida, Shin
Division of Evolution of Earth Environment, Graduate School of Social and Cultural Studies, Kyushu University

他

出版情報：Geomicrobiology Journal. 28 (2), pp.135-148, 2011-02-24. Taylor and Francis
バージョン：

Microbial processes forming daily lamination in an aragonite travertine, Nagano-yu hot spring, southwest Japan.

Tomoyo Okumura,[1] Chizuru Takashima,[2] Fumito Shiraishi,[1] Shin Nishida,[1] Kise Yukimura,[3] Takeshi Naganuma,[3] Hiroko Koike,[1] Gernot Arp[4] and Akihiro Kano[1]

[1]*Division of Evolution of Earth Environment, Graduate School of Social and Cultural Studies, Kyushu University, 744 Motooka, Nishi-ku, Fukuoka 819-0395, Japan*

[2]*Facuity of Culture and Education, Saga University, 1 Honjo-tyo, Saga, 840-8502, Japan*

[3]*Department of Enviromental Dynamics and Management, Hiroshima University, 1-4-4 Kagamiyama, Higashi-hiroshima 739-8526, Japan*

[4] *Geoscience Centre, University of Göttingen, Goldschmidtstraße 3, D-37077 Göttingen, Germany*

Running Title: Lamina-forming processes in an aragonite travertine

Address correspondence to: Tomoyo Okumura, Kyushu University, 744 Motooka, Nishi-ku, Fukuoka 819-0395, Japan. E-mail: oktomy@kyudai.jp

ABSTRACT

An aragonite travertine at Nagano-yu hot spring, SW Japan, exhibits clear sub-millimeter-order lamination that resembles ancient ministromatolites. Thirty-three hours of continuous observation showed that the lamination is formed daily with no changes in physicochemical properties except light intensity. Phylotype analysis and fluorescence *in situ* hybridization indicate that *Hydrogenophaga* sp. is dominant and concentrated in diurnal layers containing abundant extracellular polymeric substances. Growth of *Hydrogenophaga* sp. is activated in the daytime, likely due to extracellular polymeric substance production by cyanobacterial photosynthesis. Daytime development of *Hydrogenophaga*-dominant biofilms, and the concurrent inhibiting effect on aragonite precipitation, explains the daily lamination observed.

Key words: Aragonite travertine, daily lamination, cyanobacteria, *Hydrogenophaga* sp., stromatolite

INTRODUCTION

Stromatolites, macroscopically laminated benthic microbial deposit (Riding 2000), form the most reliable evidence of early life on the Earth (Allwood et al. 2006). These microbial deposits potentially hold information on the early biosphere and environments. The textural and compositional features of fossil stromatolites, however, are insufficient to understand their formation processes (Grotzinger and Rothman 1996; Riding 2000; Sumner and Grotzinger 2004).

Indeed, the study of stromatolites in modern marine settings, such as the Bahama platform (Reid et al. 1995; Reid et al. 2000) or Shark Bay (e.g. Reid et al. 2003; Burns et al. 2004), is commonly considered to provide crucial information on geomicrobiological processes that may have operated also in their fossil counterparts. One early model of lamina formation in modern marine stromatolites was proposed by Monty (1965, 1979). He suggested that in Andros Island tidal flat stromatolites lamination forms daily and is related to the phototaxic behavior of filamentous cyanobacteria growing rapidly and trapping suspended sediment grains during the daytime. Alternatively, lamination may reflect cyclic changes in the composition of the cyanobacterial community (Monty 1976). Golubic and Browne (1996) observed that the multitrichome cyanobacterial genus *Schizothrix* in subtidal stromatolites changes its growth orientation dependend on the burial by sediment. Recent investigations of similar particle-rich marine stromatolites suggest that lamination may result from a dynamic balance between carbonate particle trapping by cyanobacteria and intermittent lithification by sulfate reduction of bacteria in the biofilm (Visscher et

al. 1998; Reid et al. 2000; Andres et al. 2006).

These processes observed in modern marine stromatolites cannot be directly applied to Precambrian stromatolites, because trapping and binding of detrital particles was only a subordinate factor in their formation (Altermann 2008). Rather, they exhibit *in situ* mineral precipitation (Grotzinger and Knoll 1999). Consequently, stromatolites consisting of *in situ* precipitated minerals, such as silica sinters in Iceland and New Zealand (Konhauser et al. 2001; Jones et al. 2005b) and lithified microbial mats of saline lakes and lagoons (e.g., Vasconcelos et al. 2006) may represent closer analogs. The formation of distinct diurnal couplets of light and dark laminae by *in situ* precipitation, however, is best observed in travertines.

Travertines form in thermal spring waters containing high concentrations of calcium ions and carbon dioxide (CO_2) species. CO_2 outgases rapidly from the hot spring water because of the disequilibrium with the atmosphere, thereby inducing supersaturation of calcium carbonate minerals (Kitano 1963). Alternative definitions of the term *travertine* include thermal as well as karstwater spring deposits (e.g. Julia 1983, Pentecost 2005). In this paper, we confine the term travertine to carbonate precipitates from hot spring water, as opposed to "tufa" which is formed in water of ambient temperature (Ford and Pedley 1996). A further distinct difference between the travertines and the tufas appears are the precipitation rates: Travertines grow very quickly (several 10s cm/year; Takashima and Kano 2008), one or two order faster than tufas (several mm/year; Kano et al. 2003).

The laminated travertines reported from central Italy (e.g. Chafetz and Folk 1984), Iceland (Jones et al. 2005a), and Japan (Takashima and Kano 2008) commonly consist of dendritic calcite

crystals (dendrite; Jones et al. 2005a) intercalated with bands of microcrystalline components. The processes of such daily lamination have been interpreted in relation to microbial activities that induced calcite precipitation (Folk et al. 1985) or left organic fabrics (Guo and Riding 1992). The details of the process forming lamination was recently shown for a calcite travertine in southwestern Japan, in which the bands were formed around sunset when cyanobacteria formed glutinous biofilm on the surface as a response to decreased light intensity (Takashima and Kano 2008).

In contrast to calcite travertines, aragonite travertines have been studied focusing on mineralogical change and geochemistry (Fouke et al. 2000; Renaut and Jones 1997), but less intensively with respect to microbial communities and their effect on precipitation and fabric formation. Lamination is also common in aragonite travertines, but its microtextures differ from those of calcite laminated travertines (e.g., Kano et al. 2006). In this study we focus on an aragonitic travertine at Nagano-yu hot spring in Oita Prefecture, southwest Japan. The purpose of this study is to elucidate the mechanisms of lamina formation in this aragonite travertine, and to discuss this travertine type as a modern analog for ancient ministromatolites (e.g. Seong-Joo and Golubic 1999).

MATERIALS AND METHODS

Geological Setting and Study Site

Nagano-yu hot spring is located in Oita Prefecture, SW Japan (Figure 1a). A number of hot spring facilities in the Nagayu area are aligned along the Seri River, roughly corresponding to the Oita-Kumamoto tectonic line (Figure 1a). Spring water is discharged from depths of 50-250 m, where

the aquifer of weathered rhyolite is sealed by thick welded tuff of the Aso volcano (Figures 1a and 1b). This cap rock contributes to maintaining intermediate temperatures (~43^{o}C) and a high partial pressure of carbon dioxide (PCO_2 ~800 matm at vent; Kano et al. 2006). Isotopic studies indicated that the hot spring water in this area is meteoric in origin (Yamada et al. 2005), and that heat and CO_2 came from active Kuju volcanoes located 10 km northwest of Nagayu (Iwakura et al. 2000). The bedrock in this area consists of volcanic rocks lacking calcareous rocks (Figure 1b). This setting differs from other travertine sites with calcareous bedrock, such as Mammoth hot spring at Yellowstone National Park, USA (Sorey and Colvard 1997), Matlock Bath in the UK (Pentecost 1999) and Egerszalok in Hungary (Kele et al. 2008).

The appearance and texture of travertines in this area vary between the different spring sites dependent on hydrological and physicochemical conditions, as well as microbial associations (Kano et al. 2006). We investigated a travertine at Nagano-yu (Figure 1a; 33^{o}04' N, 131^{o}22' E), which forms the largest mound in the area and exhibits distinct alternating laminae. It is located along a steep (30◦), 30-m-long water passage beside the Seri River (Figures 1c and 2a). The water flowing on the mound has a neutral pH and is enriched with cations (Na^+, K^+, Mg^{2+} and Ca^{2+}), anions (SO_4^{2-}, Cl^- and HCO_3^-), and dissolved CO_2 (Kano et al. 2006). The appearance of the travertines is variable depending on flow conditions. At high flow passages, they are hard and light yellow in color. At adjacent low flow sites, thick microbial mats of dark green color leave loosely consolidated deposits (Figure 2b). The rapid growth rate of the travertines shifts water passage on the mound within several months, and can change mound configurations.

Analytical Methods

To trace the cyclic laminae formation at the study site, 33 h of observation were performed from 13:30 on 23 April to 22:30 on 24 April 2006 at the center of the travertine mound (sampling point; Figure 1c). Samples of water and well-consolidated travertine were collected every 1.5 h and 3 h, respectively. The series of travertine samples were carefully collected with a chisel from the surface of 20 x 20 cm^2 covered with the same hydrological conditions. Water samples were collected from the same point immediately above the travertine sampling area. Water and air temperatures, pH of the flowing water, and light intensity were also measured every 1.5 h. Additional travertine samples were collected on 10 November 2007 for fluorescence *in situ* hybridization (FISH), 10 June 2008, and 30 May 2009 for genetic analysis near the sampling point. The texture of these samples was identical to that of the samples of April 2006.

Water Analysis

The water sampling and analysis were conducted following the same procedures of Takashima and Kano (2008). The cations (Ca^{2+}, Mg^{2+}, Na^{+}, K^{+}) were measured by atomic absorption, while the anions (Cl^{-}, NO_3^{-}, SO_4^{2-}) were measured by ion-chromatography within 3 days after the sampling. Alkalinity was immediately measured by titration with 0.05 N H_2SO_4 (Bromocresol Green-Methyl Red method) after sampling (within 30 min.). PCO_2 and saturation index for aragonite (SIa) were calculated using the equations of Plummer and Bosenberg (1982). Inorganic precipitation of carbonate mineral (PWP-rate; Plummer et al. 1978) was also calculated with the equations revised by Dreybrodt and Buhman (1991) and is expressed as a surface-controlled rate ($mol/cm^2/s^1$).

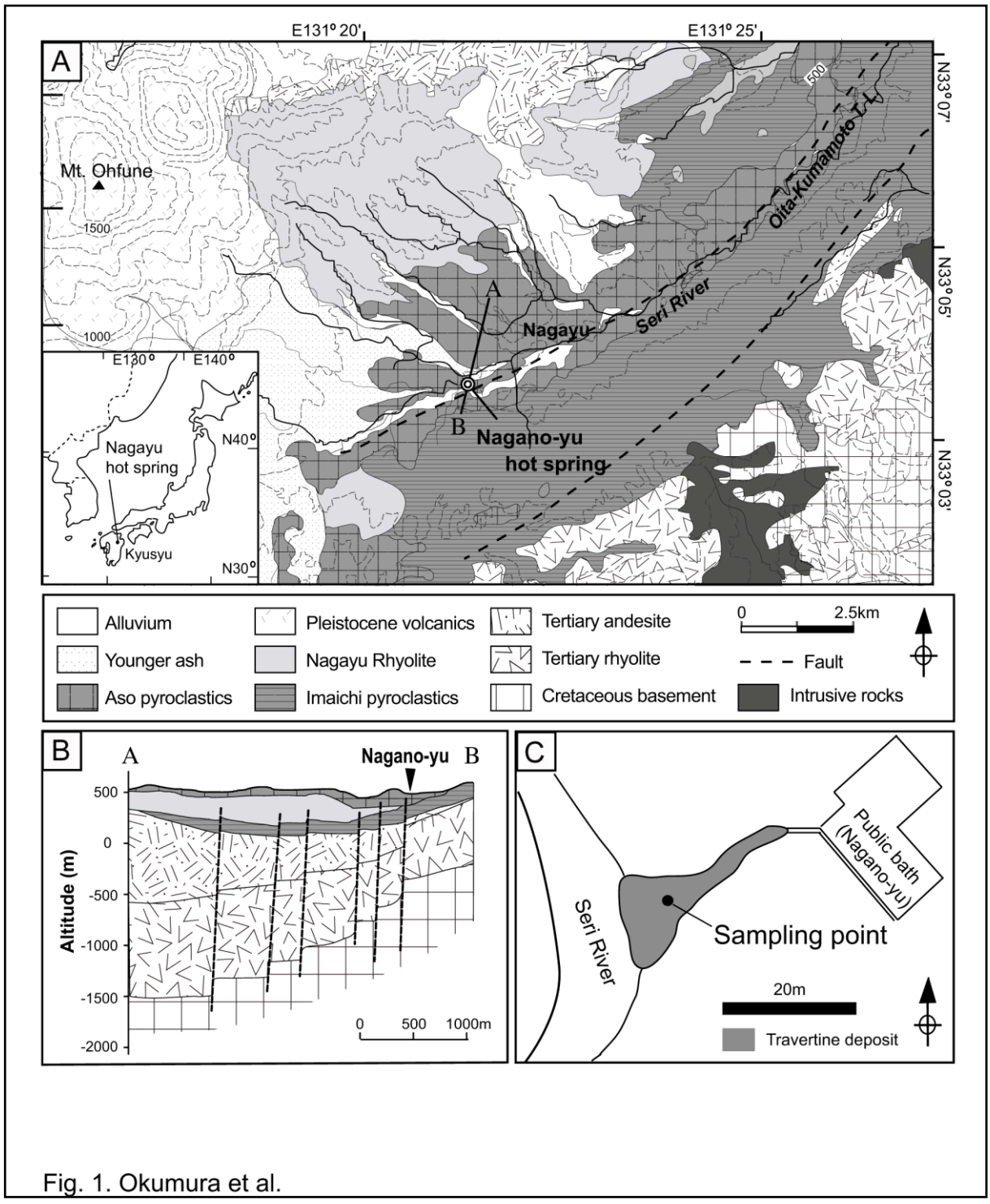

Fig. 1. Okumura et al.

Textural Observation

Sediment samples (50 cm^3) were taken from the travertine surface. Thin sections were made from the samples, which were pre-treated by three methods. (1) For textural observation, samples were dried at room temperature for several days and hardened with 50% ethanol-diluted epoxy resin (Maruto Instrument Co., Tokyo, Japan). Eleven sequenced samples collected during continuous observation were treated by this method. (2) To observe the association between cyanobacteria and aragonite crystals, samples were first soaked in 4% formaldehyde-phosphate-buffer-solution (PBS) twice for 24 h, and were then fixed in 50% ethanol-PBS to avoid destruction of bacterial cells and organic texture. To increase contrast of carbonate minerals in fluorescence microscopy, samples were stained with calcein. The fixed samples were stained in calcein solution (calcein saturated in 50% ethanol) for 30 min, and embedded with LR White resin (London Resin Co., Basingstoke, UK). Three samples collected in December 2007 were treated with this method; two thin sections were made from each sample. (3) To show extracellular polymeric substances (EPS) consisting of carbohydrates, proteins and acidic sugars (Sutherland 1990) in sections, samples were stained with toluidine blue O. Samples were fixed as in the above method, and stained in solution (7.3 g/L toluidine blue O, 2.3 g/L fuchsin in 30% ethanol) at least 30 min., washed with distilled water and then with 99% ethanol, and embedded with LR White resin. Five samples collected in 2007 were treated with this method; two thin sections were made from each sample. The samples were sliced perpendicular to the lamination and observed with optical and fluorescence microscopes.

Three-dimensional fabrics of the sediment samples were observed with a scanning electron

microscope (SEM; JOEL JXA-8200). The samples were etched by ethylene-di-amine-tetra-acetic acid (EDTA) and dried at room temperature before observation.

Fig. 2. Okumura et al.

Genomic Analysis

To identify prokaryotic taxa that potentially influence lamina formation, 16S rRNA gene sequencing was performed on clones retrieved from bulk DNA extracts of travertine samples. For genomic analysis, the samples from the travertine surface were collected in the daytime, immediately soaked into 99% ethanol and kept cool (~4^{o}C) during the transportation. Approximately 200 mg of the uppermost sample layers (~5-mm depth) were scraped with a dental drill and decalcified overnight

with 0.5 M EDTA 2Na (pH = 8). The solution was changed several times. The cell pellet was then collected by centrifuge and cleaned with sterilized distilled water.

Total DNAs were extracted with the QIAamp® DNA Micro Kit (QIAGEN, Hilden, Germany). Near-full-length sequences (~1400 bp) of the 16S rDNA gene were amplified by polymerase chain reaction (PCR) with the bacteria-specific 27F forward primer (5'-AGAGTTTGATCCTGGCTCAG-3') and the universal 1492R reverse primer (5'-GGTTACCTTGTTACGACTT-3') (DeLong 1992). The amplification was performed with a thermal cycler (TaKaRa Bio Inc., Otsu, Japan) for 30 cycles. One cycle consisted of 96^{o}C for 3 min, 94^{o}C for 30 sec, 55^{o}C for 45 sec, and 72^{o}C for 1 min with pre-heating at 96^{o}C for 3 min and post-extension at 72^{o}C for 1 min.

The amplification products were confirmed by electrophoresis (on 1.5% agarose gel, 100 V, 30 min), and subcloned using the TOPO TA Cloning Kit (Invitrogen Corp., San Diego, California, USA) into the PCR 2.1 TOPO-vector, and then transformed into the TOP 10F' strain of *E. coli*. Positive colonies were selected and screened for the correct product insert. After initial screening, the PCR products from each clone were sequenced. They were enzymatically purified (PCR Product Pre-Sequencing Kit, USB Corp., Cleveland, Ohio, USA) and direct sequencing was carried out using a Dye Terminator Cycle Sequencing Kit (Beckman Coluter Inc., Fullerton, California, USA), according to the manufacturer's protocol. Cycle sequencing consisted of 30 cycles of 96^{o}C for 30 sec, 60^{o}C for 45 sec, and 72^{o}C for 45 sec with pre-heating at 96^{o}C for 1 min and post-extension at 72^{o}C for 5 min. Capillary sequencing was conducted using the CEQ2000XL DNA Sequencer (Beckman

Coulter Inc.) and data were analyzed using CEQ software, Sequence Analysis ver. 2 (Beckman Coulter Inc.). Alignment of the sequence data was manually performed using MEGA 4.02 software (Tamura et al. 2007). M13F (5'-GTAAAACGACGGCCAG-3') and M13R (5'-CAGGAAACAGCTATGAC-3') primers were used for sequences to obtain ~450 bp from the 27F primer in one strand.

Sequence similarity was determined by the Basic Local Alignment Search Tool (BLAST; Altschul et al. 1997) on the National Center for Biotechnology Information (NCBI) website (http://www.ncbi.nlm.nih.gov/blast). The resulting 105 sequences were grouped into operational taxonomic units (OTU) on the basis of a nucleotide similarity > 98%. Representative sequences for each common OTU (including more than three sequences) were further sequenced with two bacteria-specific primers, 357F (5'-CTCCTACGGGAGGAGCAG-3') and 1100R (5'-GGGTTGCGCTCGTTG-3') (Lane 1991) to obtain near-full-length sequences (~1400 bp). Chimera sequences were checked with the program CHIMERA_CHECK at the RDP II (Cole et al. 2003) and Bellerophon Server (Hugenholtz and Huber 2003). The 16S rRNA gene sequences obtained in this study were registered in the DNA Data Bank of Japan (DDBJ; GenBank accession Nos. AB518478 to AB518482 and AB548033 to AB548045).

Fluorescence *in situ* hybridization (FISH)

FISH is a widely used technique that permits the identification and quantification of a specific bacterial group (Amann et al. 1995). We applied this method to the travertine using the catalyze reporter deposition FISH (CARD-FISH) protocol proposed by Shiraishi et al. (2008) for tufa,

the freshwater stromatolite developed in karst creeks. The protocol was applied to paraffin sections of the travertines, as described below.

Paraffin section. Each 1-cm^3 travertine sample was decalcified overnight with 20% Formical-2000 (Decal Chemical, New York, USA) and embedded in paraffin following the procedures of Hoffmann et al. (2003). The samples were gradually dehydrated with 30%, 50%, 70%, 85% and 90% ethanol for 1 h each, and were finally soaked in 99% ethanol. Dehydrated samples were soaked in xylol for 2 h and embedded in paraffin at 60^{o}C. They were then consolidated at -6^{o}C and cut into 5-μm-thick sections by microtome. Paraffin sections were mounted on silane-coated slides and the paraffin was removed by rinsing with xylol twice for 15 min, then hydrated in 99%, 90%, 70% and 50% ethanol and distilled water for 2 min.

Hybridization and observation. Fluorescence signals of conventional FISH are often too weak to obtain clear images, and therefore should be intensified by CARD-FISH using tyramide signal amplification (TSA), which allows 10- to 20-fold amplification of the FISH signal (Schönhuber et al. 1997). Following the protocol of Shiraishi et al. (2008), we used oligonucleotide probes targeting *β-Proteobacteria* (5'-GCCTTCCCACTTCGTTT-3') labeled by horseradish peroxidase. The hybridized samples were enclosed in mounting media containing DAPI (4′, 6′-diamidino-2-phenylindole; Merck, Darmstadt, Germany) to estimate the ratio of the targeted bacteria to all microbial cells, and observed with a Zeiss 510 Meta confocal laser scanning microscope (CLSM). Areal counts of the probe signals were measured with Image-Pro Plus version 5.1 software (Media Cybernetics, Inc., Georgia, USA).

RESULTS

Texture of the Aragonite Travertine

The lamination in the sample from the high flow site was visible to the naked eye as alternating dark- and light-colored layers (Figure 2c). Textural differences between the two layer types were observed under the optical microscope (Figure 2d). The dark-colored layer consisted of a pile of thin (~10 μm) laminae that are here called sub-laminae. A dark-colored layer is called an L-layer (laminated layer; Figure 2d). In turn, the light-colored layer was composed of ~100-μm-height vertically extending needle crystals (needle crystal layer: N-layer; Figure 2d and Figure 3a). The two layers had almost the same thickness in an individual sample, but ranged from 100 to 250 μm depending on depositional site. SEM images showed distinct differences in crystal length between the two layer types. Sub-laminae in the L-layer consisted of rod-shaped crystals of the full length of the lamina thickness ranging from 1 to 15 μm (Figure 3a). While the N-layer consisted of longer needle-shaped crystals were about 100 μm in length (Figure 3a). Each L-layer contained 15-30 sub-laminae.

In addition to the distinct lamination consisting of L-layers and N-layers, another characteristic texture was formed by knob-shaped aggregates of various sizes (KA in Figure 3b). The aggregates were densely packed and separated by vertical cracks (VC in Figure 3b) that corresponded to cracks truncating the lamination observed in thin section (VC in Figure 2d). On a horizontal surface, the cracks and aggregation of the knobs appeared as tightly packed polygons ~500 μm in diameter (Figure 2e). SEM images showed fibrous matter adhering to the knob-shaped aggregates, likely

corresponding to EPS or desiccated cyanobacterial body (F in Figure 3c and 3d). Lamination was observed inside the knob aggregates (Figure 3b).

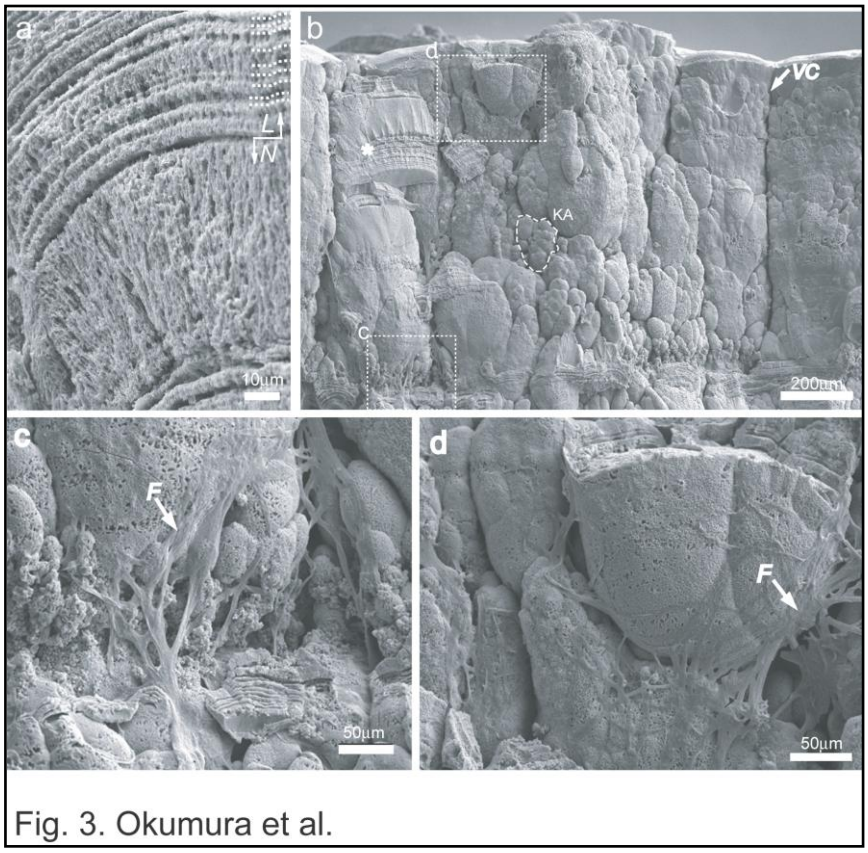

Fig. 3. Okumura et al.

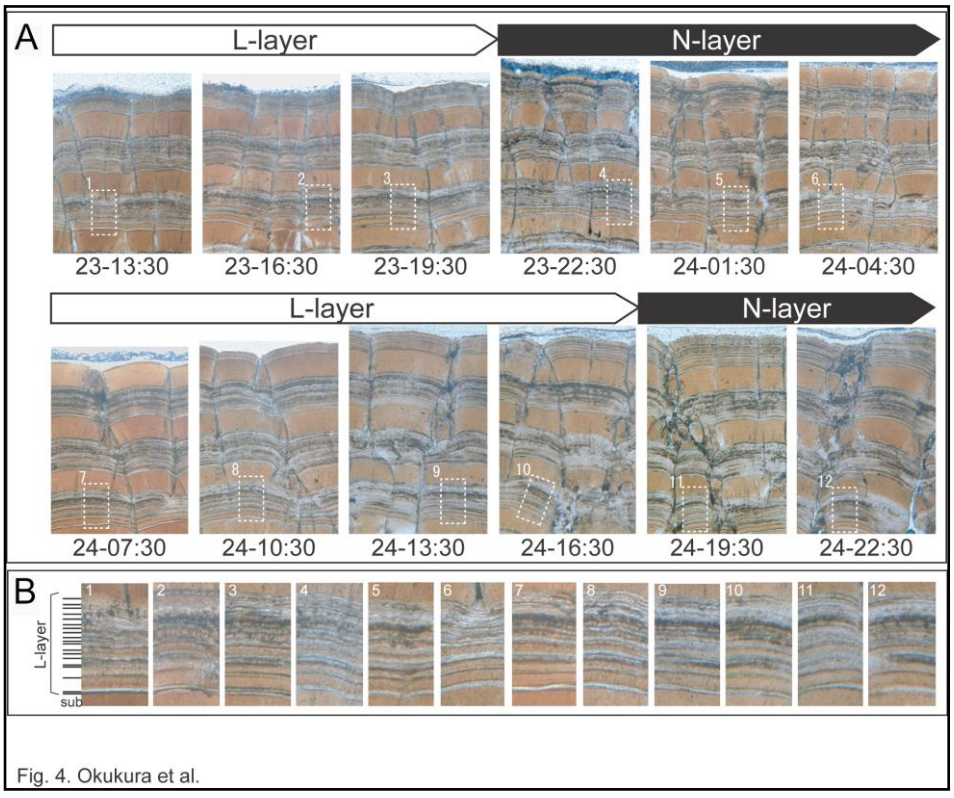

Fig. 4. Okukura et al.

Daily Changes in Texture and Physicochemical Composition

Figure 4a shows the series of thin-section images for the specimens collected every 3 h on 23-24 April 2006. This series demonstrates temporal changes in surface texture. The surfaces of samples collected during the day (at 13:30, 16:30 and 19:30 on 23 April and 7:30, 10:30, 13:30, 16:30 and 19:30 on 24 April) showed the L-layer texture, while those of samples collected at night (at 22:30 on 23 April and 1:30, 3:00 and 4:30 on 24 April) showed the N-layer texture (Figure 4a). The thin section images also provide textural details of the L-layer, which can be traceable among the samples. In the L-layer shown in Figure 4b, two relatively thick sub-laminae occur at the bottom, and the sub-lamina thickness tends to decrease upwards.

Physical and chemical properties measured at the sampling point on 23-24 April are shown in Table 1 and Figure 5. A clear day/night pattern was observed in light intensity (max. 4.95 Klux at 13:00 on 23 April, and min. 0 lux at the night time; 21:00 and 22:30 on both days, and 0:00—4:30 on 24 April) and air temperature (max. 23.0^{o}C at 15:00 on 23 April and min. 10.0^{o}C at 3:00 on 24 April). The day/night pattern was much less distinctly registered by the chemical properties. The pH ranged from 7.6 to 8.21 and was slightly higher during the day. SIa and PWP-rate changed correspondingly, and PCO_2 changed inversely to pH. The water maintained a significant level of supersaturation (SIa > 1.2) and dissolved CO_2 (PCO_2 > 16 matm). No day/night pattern was apparent in the concentrations of anions and cations, although Ca^{2+} and Mg^{2+} concentrations were variable.

Microbial Composition

The phylotype analysis revealed a low diversity in the travertine microbial assemblage and

domination by a single phylotype. The sequences (~450-bp) of 105 clones were obtained from the samples, and among them 80.0% (84 in 105 clones) were related to *Hydrogenophaga* sp., a member of the *β-Proteobacteria* (Figure 6). Other assemblage components were *γ-Proteobacteri*a (11.4%; 12 in 105), cyanobacteria (4.8%; 5 in 105 clones), *α-Proteobacteria* (1.9%; 2 in 105 clones), *δ-Proteobacteria* (1.0%; 1 in 105 clones) and *Spirochaetes* (1.0%; 1 in 105 clones).

The genus *Hydrogenophaga* is gram-negative and belongs to family *Comamodaceae*. Species of this genus generally exhibit rod-shaped cells of 0.3-0.6 x 0.6-5.5 μm in size with flagellate motility (Williems and Gillis 2005). Their optimal growth conditions are 30-40^{o}C at 7-8 pH (Williems and Gillis 2005), which fit well with the conditions of the Nagano-yu travertine site. 15 near-full-length (~1400bp) 16S rDNA sequences obtained in this study recognized high similarity with *Hydrogenophaga bisanensis* strain K102 (EF532793; Table2) and *Hydrogenophaga* sp. TRS-05 (AB166889; Table2). Calculated genetic distances of these clones indicated that formed an independent clade from other *Hydrogenophaga* spp. registered in GenBank (see Appendix).

The phylotypes of *γ-Proteobacteri*a are related to *Pseudomonas* sp. (11/12) and Thermomonas sp. (1/12). 4 near-full-length sequences were related to *Pseudomomas alcaligenes* (Z76653; Table 2). This species is a gram-negative, rod-shaped, and aerobic heterotroph (e.g., Anzai et al. 2000).

One sequence of the cyanobacteria was related to *Phormidium* sp. ETS-05 (98.6% similarity; AJ548503; Table 2) reported from hot spring mud in Italy (Berrini et al. 2004). The sequences of the other cyanobacterial clones were examined, but similarities were insufficient for

identification.

TABLE 1. Water chemistry of the Nagano-yu hot spring water at the sampling point (Figures 1c and 2a).

Date	Time	Lumi	T air	T water	pH	PCO_2	SIa	PWP-rate	Alk	DIC	Ca^{2+}	Mg^{2+}	Na^{+}	K^{+}	Cl^{-}	SO_4^{2-}
		(Lux)	(^oC)	(^oC)		(matm)			(mM)	(mM)	(mg/L)	(mg/L)	(mg/L)	(mg/L)	(mg/L)	(mg/L)
23 Apr	13:30	4950	22.4	35.1	8.10	18.5	1.7	11.9	40.0	39.96	167	278	456	78	164	509
	15:00	4106	23.0	35.7	8.13	17.3	1.8	12.8	39.8	39.63	175	286	495	83	171	522
	16:30	3500	21.0	34.0	8.01	22.2	1.6	9.9	39.8	39.93	158	291	488	82	169	520
	18:00	370	16.0	33.8	7.64	53.1	1.4	6.0	40.3	41.55	172	313	513	84	181	563
	19:30	1	14.2	32.6	7.81	34.4	1.5	6.9	39.0	39.73	153	286	493	82	173	539
	21:00	0	13.5	36.8	7.83	34.6	1.4	6.3	38.8	39.36	130	299	493	82	167	518
	22:30	0	13.5	34.4	7.68	49.0	1.3	5.2	40.0	41.14	144	296	516	85	173	542
24 Apr	0:00	0	12.0	35.3	7.70	46.2	1.3	5.2	39.0	40.03	136	268	501	83	166	518
	1:30	0	11.2	36.0	7.78	36.1	1.4	6.1	36.4	37.11	142	315	531	87	181	735
	3:00	0	10.0	35.8	7.71	42.8	1.3	4.8	36.5	37.43	129	305	524	84	175	546
	4:30	0	8.9	35.5	7.58	61.2	1.2	3.1	38.7	40.16	117	279	519	84	168	516
	6:00	120	8.1	34.8	7.71	45.3	1.3	4.4	39.2	40.21	121	299	531	85	172	538
	7:30	770	9.8	32.7	7.73	41.1	1.3	4.6	38.7	39.64	124	275	509	82	160	496
	9:00	960	10.2	34.7	7.86	30.7	1.4	5.8	37.5	38.04	122	298	524	83	171	537
	10:30	1500	12.1	35.6	7.68	46.7	1.2	3.8	37.3	38.30	116	315	524	83	170	534
	12:00	3500	16.0	35.4	7.80	36.0	1.4	6.1	38.5	39.20	134	305	526	84	169	532
	13:30	3700	19.0	34.2	8.13	16.2	1.6	8.0	37.5	37.41	118	279	526	92	173	531
	15:00	2700	19.8	34.0	7.75	38.4	1.3	4.7	36.5	37.35	122	278	521	85	173	539
	16:30	2100	20.5	34.3	7.72	40.0	1.2	3.5	35.1	36.00	104	283	511	82	169	527
	18:00	1210	13.8	33.6	7.73	43.1	1.4	5.4	40.3	41.22	137	273	529	84	175	541
	19:30	3	11.8	33.2	7.88	29.5	1.4	6.0	39.0	39.46	125	315	524	84	171	532
	21:00	0	10.5	34.4	7.75	39.2	1.3	4.6	37.5	38.35	120	331	521	83	172	545
	22:30	0	10.5	37.2	7.79	39.6	1.4	6.0	40.3	41.04	130	286	526	85	170	532

Notes: Lumi = luminosity; T = temperature; Alk = alkalinity; DIC = dissolved inorganic carbon; SIa = saturate index for aragonite. PWP-rate is expressed in 10^{-10}M, cm^{-2}, sec^{-1}.

Microbial Distribution

A distinct abundance of microbial cells in the L-layer was shown by DAPI and CARD-FISH signals (Figures 7a and 7b), using the probe for *β-Proteobacteria*. Comparison of the two image types identified that 75-80% of the bacterial cells were *β-Proteobacteria* (Figures 7a to 7d). These cells were rod-shaped of approximately 1 x 2 μm in size (Figures 7c and 7d). The bacterial cells were horizontally aligned and distributed in an area 100-150 μm thick (Figures 7a and 7b). The fabric of this cell alignment likely corresponds to the sub-laminae of the L-layer (Figures 7c and 7d).

The results of toluidine blue O staining showed EPS concentrations in the spaces along the sub-laminae of the L-layer (Figure 7e), similar to the distribution of *β-Proteobacteria* as mentioned

above. The vertical cracks were also stained, which is consistent with SEM images showing fibrous substances in these locations (Figures 3c and 3d).

Fluorescence images of the calcein-stained samples showed the distribution pattern of filamentous cyanobacteria in the travertine (Figure 7f). Filamentous autofluorescence 2 μm in diameter occurred in the cracks, but did not form a biofilm on the travertine surface as reported for calcite travertine (Takashima and Kano 2008). Weak autofluorescences were observed in the FISH image (AF in Figure 7b) and stained by DAPI (Figure 7a). It is likely originating from cyanobacteria.

TABLE 2. Relatives of > 98% similarity with the ~1.4kbp 16S rDNA sequences obtained from the aragonite travertine at Nagano-yu hot spring.

Type sequence (no. of clone)	**Accecion no.**	**Phylogenetic group**	**Closest match** (Accetion no.)	**Similarity** (%)
H3-9 (10)	AB518481	*β-Proteobacteria*	*Hydrogenophaga bisanensis* strain K102 (EF532793)	98.5
H3-4 (5)	AB548038	*β-Proteobacteria*	*Hydrogenophaga* sp. TRS-05 (AB166889)	98.5
H1-24 (4)	AB518479	*γ-Proteobacteria*	*Pseudomonas alcaligenes* (Z76653)	98.6
H1-5 (1)	AB518478	Cyanobacteria	*Phormidium* sp. ETS-05 (AJ548503)	98.6

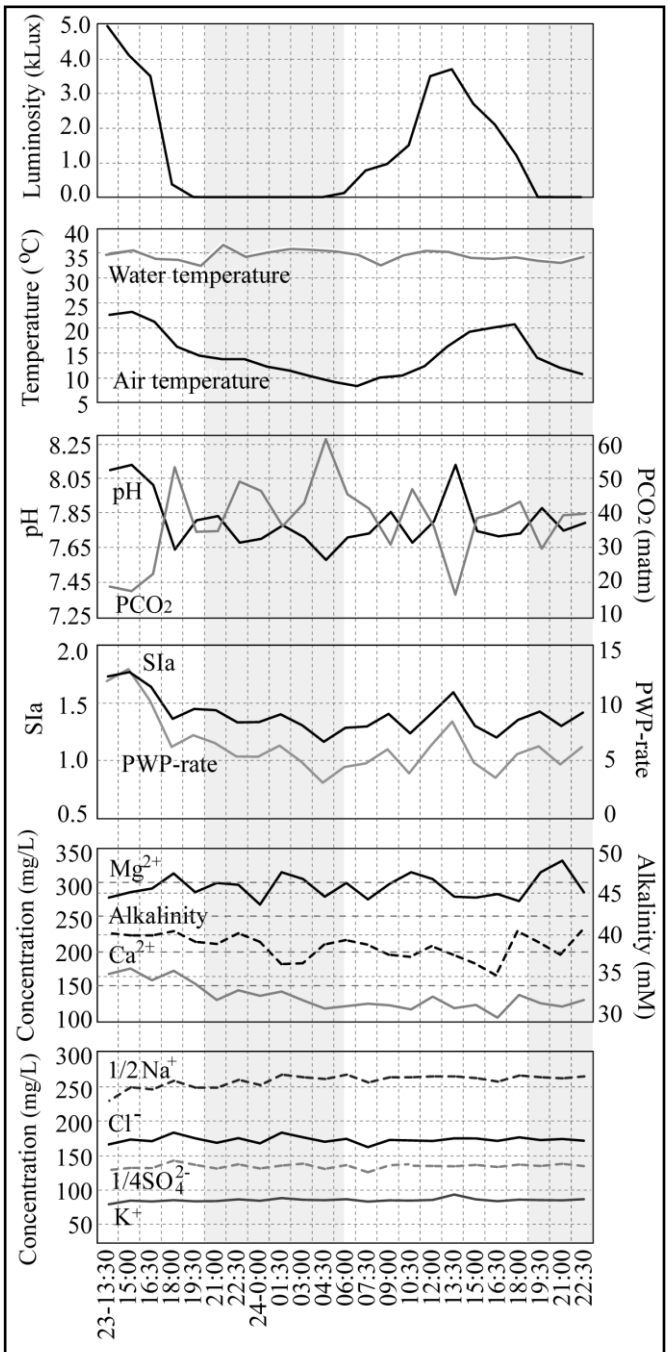

Fig. 5. Okumura et al.

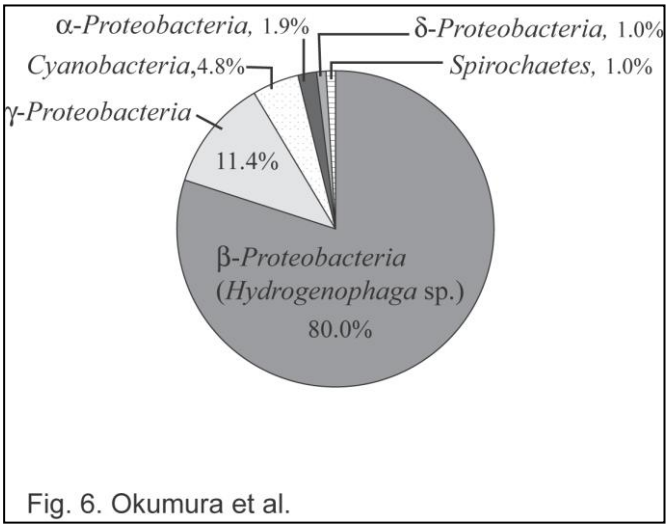

Fig. 6. Okumura et al.

DISCUSSION

The Process of Daily Lamination in the Nagano-yu Travertine

The series of thin section images for the 11 specimens collected in April 2006 showed

temporal changes in surface texture, and confirmed daily lamination consisting of daytime L-layer formation and nighttime N-layer formation (Figure 4a). The textural difference between these layers indicated different manners of crystal growth. Long aragonite needles in the N-layer document continuous mineral precipitation during the night, while short aragonite rods in sub-laminae of the L-layer indicate that the crystal growth was discontinuous during the day time and variable from time to time (Figure 4b).

In spite of clear day/night differences in texture, no significant day/night patterns were found in the water chemistry associated with carbonate precipitation. The maximum values of SIa and PWP-rate were recorded at midday, indicating a higher potential for carbonate precipitation during the day. These higher values were associated with lower PCO_2, and could be the result of CO_2 removal by photosynthesis or more active degassing. However, the effect of these chemical trends was insignificant for textural formation, as shown by similar growth rates for the diurnal L-layer and nocturnal N-layer. Daily lamination processes thus appear not to be associated with the bulk water chemistry. The textural difference between the day and night laminae is due to microbial processes associated with the daily rhythms of photosynthesis.

In this study, we found evidence of microbial activities in the travertine, including the presence of EPS stained with toluidine blue O (Figure 7e) and the abundance of *β-Proteobacteria* (Figure 7a to 7d) and *Hydrogenophaga* sp. (Table 2).

The primary material of daily lamination could be EPS. The influence of EPS on carbonate precipitation has been variously interpreted by processes such as inhibition by Ca^{2+} absorption (Arp et

al. 1999a, 1999b), promotion by provision of nucleation sites (Arp et al. 2003), and promotion by microbial EPS degradation that releases HCO_3^- and pre-bound Ca^{2+} (Dupraz et al. 2004). EPS concentrated in the L-layers may have inhibited crystal growth on the travertine surface and resulted in smaller rod-shaped crystals. The primary EPS producer was cyanobacteria, the only photoautotroph recognized in our phylotype analysis.

The dominant microbe identified in this study was *Hydrogenophaga* sp. (Table 2 and Figure 6). This bacterial genus can be a heterotroph or a chemoautotroph using H_2 as an energy source (Williems and Gillis 2005). Our observations indicated that the bacteria we identified are likely heterotrophs consuming EPS as an energy source: If they were chemoautotrophs using H_2 in the hot spring water, they would grow at night and should thus occur in the N-layer. The most closely related bacteria (*H. bisanensis*, EF532793; Table 2) is also a heterotroph (Yoon et al. 2008). The heterotrophic community was dominated by *Hydrogenophaga* sp. and accompanied by the aerobic heterotrophic *Pseudomonas* (e.g. Anzai et al. 2000).

Piles of sub-laminae in the L-layer formed during presence and degradation of EPS. It is suggested that these EPS, primarily produced by cyanobacteria, initially rather inhibit than promote aragonite precipitation. However, their degradation, breakdown of inhibition by the observed periodic blooms of the heterotrophic community (dominated by *Hydrogenophaga*) (Figure 7b and 7d) and contemporary release of Ca^{2+} is interpreted here to drive the precipitation of single sub-laminae. The following decline in heterotrophs cell numbers on the travertine surface would allow renewed accumulation of EPS on the travertine surface and, hence, temporary inhibition of aragonite

precipitation. The duration of this cycle is estimated to be ~30 min., based on the number of sub-laminae (15-30) in an L-layer. Our investigation of the Nagano-yu travertine thus indicates that the microbial requirement for daily lamination is the co-existence of EPS-consuming heterotrophs and EPS-producing phototrophs.

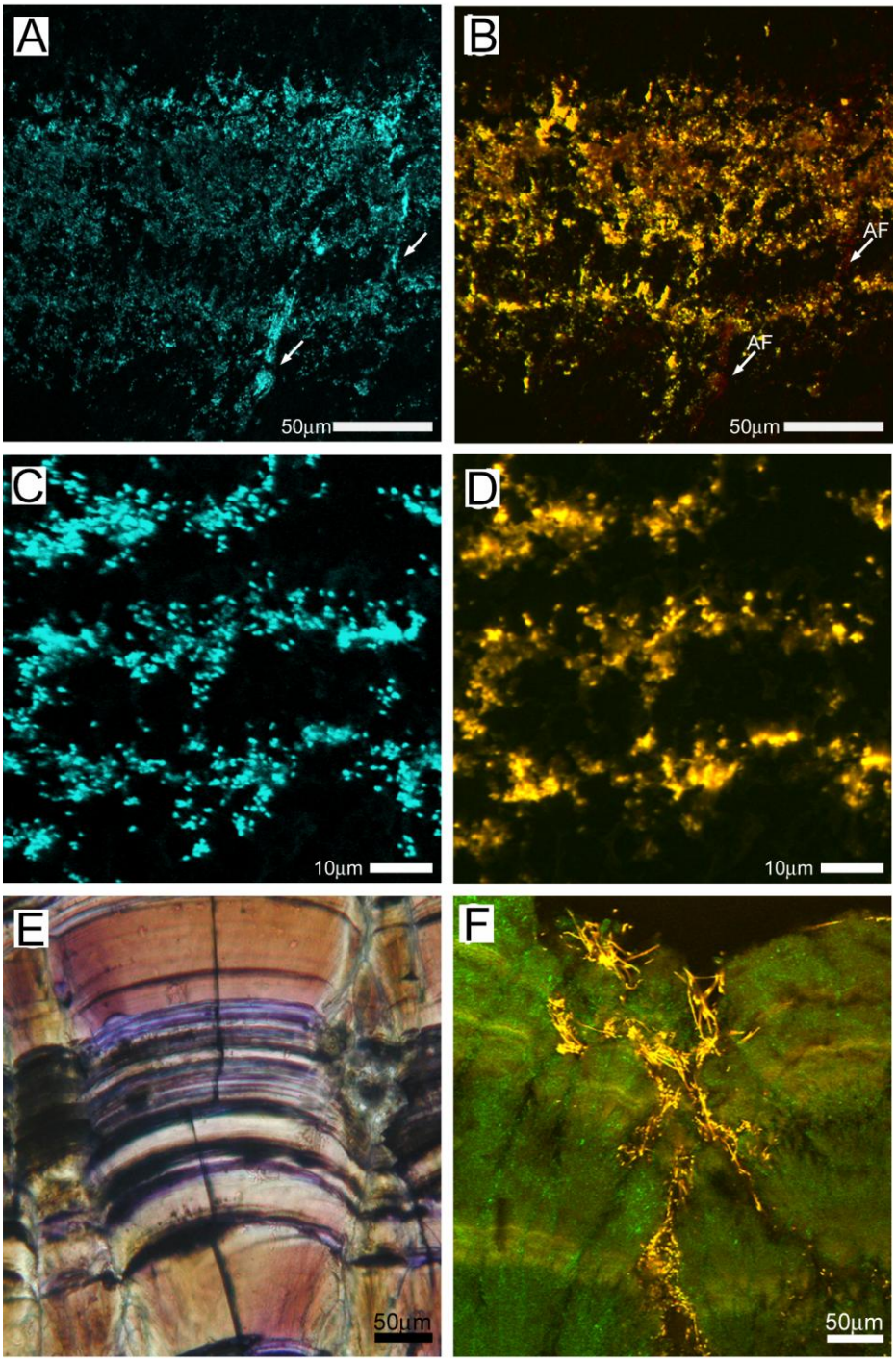

(Fig.7)

Comparison with Previous Models

The model for daily lamination of the Nagano-yu travertine proposed in this paper differs from models previously suggested for calcitic travertines. Folk et al. (1985) suggested that day/night replacement of the bacterial community on the travertine surface was responsible for daily lamination in calcite travertine in central Italy; cyanobacteria induced daytime calcite precipitation, while heterotrophic bacteria caused a microcrystalline layer at night. Also from central Italy, Guo and Riding (1992) found thin aragonite layers in calcite travertine and considered that the aragonite layers were formed in the daytime under higher supersaturation induced by microbial photosynthesis. Recently, 30-h continuous observation by Takashima and Kano (2008) showed that cyanobacterial phototaxic behavior built biofilm around sunset on a calcite travertine surface in Japan, which trapped suspended particles.

The distinct difference between these examples and the Nagano-yu travertine lies in the distribution of cyanobacteria. These bacteria occurred on the surface of calcite travertines, while they are limited to vertical cracks in the Nagano-yu travertine (Figure 7f). This difference relates to the mineralogical processes responsible for the difference in travertine texture. Dendrite, an aggregation of rhomboidal crystals with a branching fabric, is a general texture in calcite travertines (e.g., Jones et al. 2005a) that leaves empty internal spaces and a rugged surface (Takashima and Kano 2008). These textural characteristics provide substrates for settlement of filamentous cyanobacteria. In the aragonite travertine, cyanobacteria probably occur only in cracks because the smooth surface formed by tightly-packed aragonite needles or rods prevents the settlement of cyanobacterial filaments.

Cyanobacteria have been considered the microorganisms responsible for daily lamination because of their light dependency. Previous models have focussed on direct roles for the cyanobacterial community, such as the trapping of detrital or suspended particles (Takashima and Kano 2008) and alteration of the ambient chemical condition through photosynthesis (Folk et al. 1985; Guo and Riding 1992). This study suggests an indirect role for cyanobacteria, the secretion of EPS that triggers *Hydrogenophaga*-dominant biofilm on the surface.

The Mg/Ca molar ratio (~3) of the Nagano-yu hot spring water is exceptionally high for travertine site (e.g. Pentecost 2005). The high Mg/Ca ratio inhibits calcite crystal growth (Wada et al. 1999; Hardie 2003; Xie et al. 2007), although travertine mineralogy can be controlled a complex set of variables (Renaut and Jones 1997). We examined only one study site in this study; additional studies of aragonite and calcite travertines with similar fabrics (e.g., Lavrushin et al. 2006) are necessary to test the wider applicability of this model.

A Potential Analog for Ancient Stromatolites

The regular, parallel and alternate lamination of the Nagano-yu aragonite travertine is similar to that of ministromatolites found in Neoarchean (Sumner and Grotzinger 2004) to Mesoproterozoic (Hofmann and Jackson 1987; Cao 1991; Seong-Joo and Golubic 1999; Sharma and Sergeev 2004) components of Precambrian strata. This ministromatolite lamination consists of large-grained light and fine-grained, organic-rich dark layers with thicknesses of ~10 μm (e.g., first-order lamination in Cao 1991; Hoffmann and Jackson 1987; Seong-Joo and Golubic 1999). These layers resemble the lamination of the Nagano-yu travertine (Figure 2d), with one order smaller

geometry. Silicified material from Mesoproterozoic strata in North China preserves filamentous and coccoid microbes considered to be cyanobacteria (Seong-Joo and Golubic 1999). Another similarity in the fabrics is exhibited by filamentous microfossils in spaces between fan-shaped structures (Seong-Joo and Golubic 1999), indicating that the microbes did not form a film on the surface of fine lamination. We observed similar characteristics in the Nagano-yu travertine. Our model provides information of daily lamina formation for interpreting the uncertainty in the time-significance of stromatolite lamination (e.g. Hofmann 1973).

Without early silicification, Precambrian stromatolites seldom retain traces of microbes. Cyanobacteria are commonly calcified and preserved in Paleozoic-Mesozoic limestone, but are uncommon in Precambrian deposits. The Precambrian stromatolites and the Nagano-yu travertine are also similar because they lack calcified cyanobacteria. These bacteria were not calcified in the Nagano-yu travertine because: 1) they inhibited calcification by means of EPS secretion; and 2) cyanobacterial photosynthesis did not induce calcification. The latter assumption can be ascribed to buffering CO_2-assimilation by high dissolved inorganic carbon concentrations (Arp et al. 2001), i.e., conditions that may also applied to Neoarchean to Mesoproterozoic seawater.

The textual resemblance to the Nagano-yu travertine may also point to an aragonitic mineralogy of the Precambrian ministromatolites, which provides another constraint on chemical composition of ancient seawater. The Nagano-yu travertine precipitated from the water of high Mg/Ca molar ratio (~3) and neutral pH. Hardie (2003) predicted that secular variation in the Precambrian shallow-water carbonate mineralogy had been primary controlled by Mg/Ca ratio of sea water;

favorable for aragonite precipitation with a ratio more than 2.

To our knowledge, this is the first model presented for daily lamination of aragonite travertines. It differs from previous models for calcite travertines and several modern stromatolites. Comparing the thickness of laminations between the Nagano-yu travertine and Precambrian ministromatolites, ancient seawater was less supersaturated than the hot spring, but still supported rapid precipitation of carbonate minerals, which cannot be observed in modern seawater. Further investigation of ancient stromatolites to test possible daily lamination may aid understanding of Precambrian seawater conditions.

ACKNOWLEDGEMENTS

We thank two anonymous reviewers for giving a number of constructive comments that improved the manuscript. We are grateful to Yasuhiro Shibata for SEM analysis, Hayami Ishisako for preparing thin sections and Yukihisa Kudo for providing geological information of Nagayu area. Support and information were kindly provided by the owners of the Nagano-yu hot spring. 33 h observations were conducted with supporting of the laboratory members. We thank Dr. Jennifer Piehl (Wight Science Right, Nevada, USA) for editing English. This study was supported by grants-in-aid from the Japanese Ministry of Education and Science (to TO and AK), and the Program for Enhancing Systematic Education in Graduate Schools of Hiroshima University.

REFERENCES

Allwood AC, Walter MR, Kamber BS, Marshall CP & Burch IW, 2006. Stromatolite reef from the Early Archaean era of Australia. Nature 441:714—718.

Altermann W. 2008. Accretion, trapping and binding of sediment in Archean stromatolites — morphological expression of the antiquity of life. Space Sci Rev 135:55—79.

Altschul SF, Madden TL, Schaffer AA, Zhang J, Zhang Z, Miller W, Lipman DJ. 1997. Gapped BLAST and PSI-BLAST: a new generation of protein database search programs. Nucleic Acids Res 25:3389—3402.

Amann RI, Ludwig W, Schleifer KH. 1995. Phylogenetic identification and *in situ* detection of individual microbial cells without cultivation. Microbiol Rev 59:143—169.

Andres MS, Sumner DY, Reid RP, Swart PK. 2006. Isotopic fingerprints of microbial respiration in aragonite from Bahamian stromatolites. Geology 34:973—976.

Anzai Y, Kim H, Park JY, Wakabayashi H, Oyaizu, H. 2000. Phylogenetic affiliation of the pseudomonas based on 16S rRNA sequence. Int J Syst Evol Microbiol 50:563—589.

Arp G, Reimer A, Reitner J. 2001. Photosynthesis-induced biofilm calcification and calcium concentrations in Phanerozoic ocean. Science 292:1701—1704.

Arp G, Thiel V, Reimer A, Michaelis W, Reitner J. 1999a. Biofilm exopolymers control microbialite formation at thermal springs discharging into the alkaline Pyramid Lake, Nevada, USA. Sediment. Geol 126:159—176.

Arp G, Reimer A, Reitner J. 1999b. Calcification in cyanobacterial biofilms of alkaline salt lakes. Eur J Phycol 34:393-403.

Arp G, Thiel V, Reimer A, Reitner J. 2003. Microbialite formation in seawater of increased alkalinity, Satonda Crater Lake, Indonesia. J Sediment Res 73:105—127.

Berrini CC, De Appolonia F, Dalla Valle L, Komarek J, Andreoli C. 2004. Morphological and molecular characterization of a thermophilic cyanobacterium (Oscillatoriales) from Euganean Thermal Springs (Padua, Italy). Arch Hydrobiol Suppl Algol Stud. 133:73—85.

Burne RV, Moore LS. 1987. Microbialites: Organosedimentary deposits benthic microbial communities. Palaios 2:241-254.

Burns BP, Goh F, Allen M, Neilan BA. 2004. Microbial diversity of extant stromatolites in the hypersaline marine environment of Shark Bay, Australia. Environ Microbiol 6:1096-1101.

Cao R. 1991. Origin and order of cyclic growth patterns in matministromatolite bioherms from the Proterozoic Wumishan formation, North China. Precambrian Res. 52:167—178.

Chafetz HS, Folk RL. 1984. Travertines; depositional morphology and the bacterially constructed constituents. J Sediment Res 54:289—316.

Cole JR, Chai B, Marsh TL, Farris RJ, Wang Q, Kulam SA, Chandra S, McGarrell DM, Schmidt TM, Garrity GM, Tiedje JM. 2003. The Ribosomal Database Project (RDP-II): previewing a new autoaligner that allows regular updates and the new prokaryotic taxonomy. Nucleic Acids Res 31:442–443.

Dreybrodt W, Buhmann D. 1991. A mass transfer model for dissolution and precipitation of calcite

from solutions in turbulent motion. Chem Geol 90:107–122.

DeLong EF. 1992. Archaea in coastal marine environment. Proc Nat Acad Sci USA 89:5685—5689.

Dupraz C, Visscher PT, Baumgartner LK, Reid RP. 2004. Microbe-mineral interactions: early carbonate precipitation in a hypersaline lake (Eleuthera Island, Bahamas). Sedimentology 51:745—765.

Folk RL, Chafetz HS, Tiezzi PA. 1985. Bizarre forms of depositional and diagenetic calcite in hot-spring travertines, central Italy. In: Scheiderman N, Harris PM, editors. Carbonate Cements. SEPM Special Publication No.36. Tulsa: Society for Sedimentary Geology. p. 349—369.

Ford TD, Pedley M. 1996. A review of the tufas and travertine deposits of the world. Earth Sci Rev 41:117-175.

Fouke BW, Farmer JD, Des Marais DJ, Pratt L, Sturchio NC, Burns PC, Discipulo MK. 2000. Depositional facies and aqueous-solid geochemistry of travertine-depositing hot springs (Angel Terrace, Mammoth hot springs, Yellostone national park, USA. J Sediment Res 70:565-585

Golubic S and Browne KM. 1996. *Schizothrix gebeleinii* sp. nov. builts subtidal stromatolites, Lee Stocking Islands, Bahamas. Algol Stud 83:273—290.

Grotzinger JP, Knoll AH. 1999. Stromatolites in Precambrian carbonate: Evolutionary mileposts or environmental dipsticks? Annu Rev Earth Planet Sci 27:313—358.

Grotzinger JP, Rothman, DH. 1996. An abiotic model for stromatolite morphogenesis. Nature 383:423—425.

Guo L, Riding R. 1992. Aragonite laminae in hot water travertine crust, Rapolano, Italy.

Sedimentology, 39, 1067–1079.

Hardie LA. 2003. Secular variations in Precambrian seawater chemistry and the timing of Precambrian aragonite seas and calcite seas. Geology 31:785—788.

Hoffmann F, Janussen D, Dröse W, Arp G, Reitner J. 2003. Histological investigation of organisms with hard skeletons: a case study of siliceous sponges. Biotechnology and Histochemistry 78:191—199.

Hofmann HJ. 1973. Stromatolites: characteristics and utility. Earth Sci Rev 9: 339–373.

Hofmann HJ, Jackson GD. 1987. Proterozoic ministromatolites with radial-fibrous fabric. Sedimentology 34: 963—971.

Hugenholtz P, Huber T. 2003. Chimeric 16S rDNA sequences of diverse origin are accumulating in the public databases. Int J Syst Evol Microbiol 53:289—293.

Iwakura K, Ohsaw S, Takamatsu N, Oue K, Notsu K, Yusa Y, Imahashi M. 2000. Origin of carbon dioxide discharged from Nagayu Hot Spring, Oita Prefecture, Japan. Onsen Kagku 50:86—93 (Japanese with English abstract).

Jones B, Renaut WR, Owen BR, Torfason H. 2005a. Growth patterns and implications of complex dendrites in calcite travertines from Lýsuhóll, Snæfellsnes, Iceland. Sedimentology 52:1277—1301.

Jones B, Renaut RW, Konhauser KO. 2005b. Genesis of large siliceous stromatolites at Frying Pan Lake, Waimangu geothermal field, North Island, New Zealand. Sedimentology 52:1129—1252.

Julia R. 1983. Travertines. In: Scholle PA, Bebout DG, Moore C editors. Carbonate Depositional Environments. Am Ass Petrol Geol Mem 33:64-72.

Kele S, Demeny A, Siklosy Z, Nemeth T, Toth M, Kovacs MB. 2008. Chemical and stable isotope composition of recent hot-water travertines and associated thermal waters, from Egerszalok, Hungary: Depositional facies and non-equilibrium fractionation. Sediment Geol 211:53—72.

Kano A, Matsuoka J, Kojo T, Fujii H. 2003. Origin of annual laminations in tufa deposits, southwest Japan. Palaeogeogr Palaeoclimatol Palaeoecol 191:243-262.

Kano A, Takashima C, Ohtsuka S. 2006. Hot-springs in eastern Kyushu and their related sedimentation and microbial processes. In: Ito M, Yagishita K, Matsuda H editors. 17th Internatinal Sedimentological Congress, 2006, Fukuoka. Field Excursion Guidebook FE-A10. The Sedimentological Society of Japan. 10 p.

Kitano Y. 1963. Geochemistry of calcareous deposits found in hot springs. Journal of Earth Sci Nagoya Univ 1:68—100.

Konhauser KO, Phoenix VR, Bottrell SH, Adams DG, Head IM. 2001. Microbial-silica interactions in Icelandic hot spring sinter: possible analogues for some Precambrian siliceous stromatolites. Sedimentology 48:415—433.

Lane DJ. 1991. 16S/23S rRNA sequencing. In: Stackebrandt E, Goodfellow M, editors. Nucleic acid techniques in bacterial systematics. Chichester: John Wiley & Sons. P. 115—163.

Lavrushin VY, Kuleshov VN, Kikvadze OE. 2006. Travertine of the northern Caucasus. Lithol Miner Resour 41:137—164.

Monty CLV. 1965. Recent algal stromatolites in the windward lagoon Andros Island, Bahamas. Bull Ann Soc Geol Belg 88B:269—276.

Monty CLV. 1979. Secientific Reports of the Belgian expedition on the Australian Great Barrier Reefs. 1967. Sedimentology 2. Monospecific stromatolites from Great Barrier Reef tract and their paleontological signigicance. Ann Soc Geol Belg 101:163—171.

Ono K. 1963. Geology of the Kuju district. Geological Sheet Map at 1:50,000 with explanatory text. Geol Surv Japan, 106 p (in Japanese with English abstract).

Pentecost A. 1994. Formation of laminate travertines at Bagno Vignone, Italy. Geomicrobiol J 12:239—251

Pentecost A. 1999. The origin and development of the travertines and associated thermal waters at Matlock Bath, Derbyshire. Proc Geol Assoc 110:217–232

Pentecost A. 2005. Travertine. Berlin: Springer-Verlag. 445p.

Plummer LN, Bosenberg E. 1982. The solubilities of calcite, aragonite and vaterite in CO_2-H_2O solutions between 0 and 90˚C, and an evaluation of the aqueous model for the system $CaCO_3$-CO_2-H_2O. Geochim Cosmochim Act 46:1011—1040.

Plummer LN, Wigley TML, Parkhurst DL. 1978. The kinetics of calcite dissolution in CO_2-water systems at 5˚ to 60˚ and 1.0 atm CO_2. Am J Sci 278:179—216.

Reid RP, Macintyre IG, Browne KM, Steneck RS, Miller T. 1995. Modern marine stromatolites in the Exuma Cays, Bahamas; Uncommonly common. Facies 33:1-18.

Reid RP, James NP, Macintyre IG, Dupraz CP, Burne RV. 2003. Shark Bay stromatolites: Microfabrics and reinterpretation of origin. Facies 49:299-324.

Reid RP, Visscher PT, Decho AW, Stolz JF, Bebout BM, Dupraz C, Macintyre IG, Paerl HW, Pinckney

JL, Prufert-Bebout L, Steppe TF, Des Marais DJ. 2000. The role of microbes in accretion, lamination and early lithification of modern marine stromatolites. Nature 406:989—992.

Renaut RW, Jones B. 1997. Controls on aragonite and calcite precipitation in hot spring travertines at Chemurkeu, Lake Bongoria, Kenya. Can J Earth Sci 34:801-818.

Riding R. 2000. Microbial carbonates: the geological record of calcified bacterial-algal mats and biofilms. Sedimentology 47:79–214.

Schönhuber W, Fuchs B, Juretschoko S, Amann R. 1997. Improved sensitivity of whole-cell hybridization by the combination of horseradish peroxidase-labeled oligonucleotides and tyramide signal amplification. Appl Environ Microbiol 63:3268—3273.

Seong-Joo L, Golubic S. 1999. Microfossil populations in the context of synsedimentary micrite deposition and acicular carbonate precipitation: Mesoproterozoic Gaoyuzhuang Formation, China. Precambrian Res 96:183—208.

Sharma M, Sergeev VN. 2004. Genesis of carbonate precipitate patterns and associated microfossils in Mesoproterozoic formations of India and Russia - a comparative study. Precambrian Res 134:317—347.

Shiraishi F, Zippel B, Neu TR, Arp G. 2008. In situ detection of bacteria in calcified biofilms using FISH and CARD-FISH. J Microbiol Methods 75:103—108.

Sorey ML, Colvard EM. 1997. Hydrologic investigations in the Mammoth Corridor, Yellowstone National Park and vicinity, USA. Geothermics 26:221—249.

Sumner DY, Grotzinger JP. 2004. Implications for Neoarchaean ocean chemistry from primary

carbonate mineralogy of the Campbellrand-Malmani Platform, South Africa. Sedimentology 51:1273—1299.

Sutherland IW. 1990. Biotechnology of Exopolysaccharides. Cambridge: Cambridge University Press. 163p.

Takashima C, Kano A. 2008. Microbial processes forming daily lamination in a stromatolitic travertine. Sediment Geol 208:114—119.

Tamura K, Dudley J, Nei M, Kumar S. 2007. MEGA4: Molecular Evolutionary Genetics Analysis (MEGA) software version 4.0. Mol Biol Evol 24:1596—1599.

Vasconcelos C, Warthmann R, McKenzie JA. Visscher PT, Bittermann AG, Lith YV. 2006. Lithifing microbial mats in Lagoa Vermelha, Brazil: Modern Precambrian relics? Sediment Geol 185:175-183.

Visscher PT, Reid RP, Debout BM, Hoeft S, Macinryre IG, Thompson Jr JA. 1998. Formation of lithified micritic laminae in modern marine stromatolites (Bahamas): The role of sulfur cycling. Am Mineral 83:1482—1493.

Wada N, Yamashita K, Umegaki T. 1999. Effects of carboxylic acids on calcite formation in the presence of Mg^{2+} ions. J Colloid Interface Sci 212:357—364.

Williems A, Gillis M. 2005. Genus V: *Hydrogenophaga* Williems, Busse, Goor, Pot, Falsen, Jantzen, Hoste, Gillis, Kersters, Auling and De Ley 1989, 329^{VP}. In: Brenner DJ, Kreig NP, Staley JT, Garrity GM, editors. Bergey's Manual of Systematic Bacteriology. 2nd ed. vol. 2. New York: Springer-Verlag. p. 710—716.

Xie A, Shen Y, Li X, Yuan Z, Qiu L, Zhang C, Yang Y. 2007. The role of Mg^{2+} and Mg^{2+}/amino acid

in controlling polymorph and morphology of calcium carbonate crystal. Materials Chem Physic 101:87—92.

Yamada M, Amita K, Ohsawa S. 2005. Isotope-hydrological study on formation mechanism of carbonate springs at the southeastern foothills of Kuju Volcano, central Kyushu, Japan. Onsen Kagaku 54:163—172 (Japanese with English abstract).

Yoon KS, Tsukada N, Sakai Y, Ishii M, Igarashi Y, Nishihara H, 2008. *Hydrogenophaga bisanensis* sp. nov., isolated from wastewater of a textile dye works. Int J Syst Evol Microbiol 58:393—397.